Published in final edited form as:

J Immunol. 2016 October 1; 197(7): 2816–2827. doi:10.4049/jimmunol.1600598.

Mincle Signaling Promotes Con-A Hepatitis

Stephanie H. Greco[*,1], **Alejandro Torres-Hernandez**[*,1], **Aleksandr Kalabin**[*], **Clint Whiteman**[*], **Rae Rokosh**[*], **Sushma Ravirala**[*], **Atsuo Ochi**[*], **Johana Gutierrez**[*], **Muhammad Atif Salyana**[*], **Vishnu R. Mani**[*], **Savitha V. Nagaraj**[*], **Michael Deutsch**[*], **Lena Seifert**[*], **Donnele Daley**[*], **Rocky Barilla**[*], **Mautin Hundeyin**[*], **Yuriy Nikifrov**[*], **Karla Tejada**[*], **Bruce E. Gelb**[*], **Steven C. Katz**[¶], and **George Miller**[1,#]

[*]S. Arthur Localio Laboratory, Department of Surgery, New York University School of Medicine, 550 First Avenue, New York, NY 10016

[#]S. Arthur Localio Laboratory, Department of Cell Biology, New York University School of Medicine, 550 First Avenue, New York, NY 10016

[¶]Immunotherapy Program, Roger Williams Medical Center, 825 Chalkstone Avenue, Providence, RI 02908

Abstract

Concanavalin-A (Con-A) hepatitis is regarded as a T cell-mediated model of acute liver injury. Mincle is a C-type lectin receptor (CLR) that is critical in the immune response to mycobacteria and fungi, but does not have a well-defined role in pre-clinical models of non-pathogen mediated inflammation. Since Mincle can ligate the cell death ligand SAP130, we postulated that Mincle signaling drives intrahepatic inflammation and liver injury in Con-A hepatitis. Acute liver injury was assessed in the murine Con-A hepatitis model using C57BL/6, Mincle$^{-/-}$, and Dectin-1$^{-/-}$ mice. The role of C/EBPβ and HIF-1α signaling was assessed using selective inhibitors. We found that Mincle was highly expressed in hepatic innate inflammatory cells and endothelial cells in both mice and humans. Furthermore, sterile Mincle ligands and Mincle signaling intermediates were increased in the murine liver in Con-A hepatitis. Most significantly, Mincle deletion or blockade protected against Con-A hepatitis whereas Mincle ligation exacerbated disease. Bone marrow chimeric and adoptive transfer experiments suggested that Mincle signaling in infiltrating myeloid cells dictates disease phenotype. Conversely, signaling via other CLRs did not alter disease course. Mechanistically, we found that Mincle blockade decreased the NF-κβ related signaling intermediates, C/EBPβ and HIF-1α, both of which are necessary in macrophage-mediated inflammatory responses. Accordingly, Mincle deletion lowered production of nitrites in Con-A

Send Correspondence to: George Miller, MD, Departments of Surgery and Cell Biology, New York University School of Medicine, 450 East 29th Street, East River Science Park, Room 843F, New York, NY 10016, Tel: (646) 501-2208, Fax: (212)-263-6840, george.miller@nyumc.org.

[1]SHG and ATH contributed equally to this work

Author Contributions: Stephanie H. Greco and Alejandro Torres-Hernandez designed research studies, conducted experiments, acquired and analyzed data, and contributed to writing manuscript. S. Rae Rokosh performed experiments and analyzed data. Sushma Ravirala, Aleksandr Kalabin, Muhammad Atif Salyana, Clint Whiteman, Vishnu Mani, and Savitha V. Nagaraj performed experiments. Michael Deutsch, Lena Seifert, Donnele Daley, Rocky Barilla, Yuriy Nikifrov, and Mautin Hundeyin contributed to experimental design and planning and performing experiments. Steven Katz offered data analysis and critical review. George Miller is principal investigator with oversight of experimental design, data analysis and interpretation, and manuscript production.

The authors have no conflicts of interest to declare.

hepatitis and inhibition of both C/EBPβ and HIF1-α reduced the severity of liver disease. Our work implicates a novel innate immune driver of Con-A hepatitis and, more broadly, suggests a potential role for Mincle in diseases governed by sterile inflammation.

Keywords

pattern recognition receptor; inflammation; liver

Introduction

Acute liver injury (ALI) is a significant public health problem which can result in jaundice, coagulopathy, hepatic encephalopathy, and multisystem organ failure[1–3]. There are many etiologies of acute liver injury including acetaminophen (APAP) overdose, viral or alcoholic hepatitis, acute fatty liver of pregnancy, and various other drug-induced and idiopathic causes. ALI accounts for approximately 6% of liver-related deaths in the United States, and approximately 7% of orthotopic liver transplants[4]. Murine modeling has helped elucidate a number of diverse pathogeneses of ALI. Concanavalin-A (Con-A) is a plant-derived lectin which induces liver inflammation in mice upon systemic administration, and is a well-studied and validated animal model of acute liver injury[5]. Con-A is thought to bind and distort MHC II moieties on resident liver APCs, which in-turn stimulate $CD4^+$ T cells to proliferate, leading to cytokine secretion and an insidious cycle of inflammation and hepatocellular injury[6].

Mincle is a C-type lectin trans-membrane pattern recognition receptor, which is required for the innate immune response to mycobacterial and fungal pathogens[7]. Mincle is expressed on innate immune cells including macrophages, dendritic cells, and neutrophils. Mincle signaling occurs through its association with ITAM-containing FC receptor γ (FCRγ) leading to recruitment of the CARD9 adaptor protein and phosphorylation of Syk, resulting in potent inflammatory responses, including the secretion of TNFα and IL-6[7]. Importantly, besides binding fungal- or mycobacterial-derived PAMPs, Mincle has recently been shown to be capable of *in vitro* ligation of spliceosome-associated protein 130 (SAP130), a nuclear protein which is released as an endogenous product of non-apoptotic cell death[8]. Further, we reported that Mincle ligation by SAP130 can modulate inflammation *in vivo* in the pancreatic tumor microenvironment [9].

We have recently reported that necroptosis, an organized form of cellular necrosis, is a primary mode of cell death in acute liver injury, and specifically in the murine Con-A model[10]. Therefore, we postulated that Mincle may play an important role in the pathogenesis of this disease by ligating products of hepatocyte cell death, thereby augmenting inflammation. In this study we show that Mincle, its ligand SAP130, and associated downstream signaling intermediates are upregulated in Con-A hepatitis in mice, and that Mincle deletion or blockade is protective against disease progression. Further, we found that Mincle signaling governs inflammation in Con-A hepatitis by modulating expression of critical pro-inflammatory and regulatory chemokines via the transcription factors C/EBPβ and HIF-1α. Our work thus implicates a novel innate immune mediator of

Con-A hepatitis which has important ramifications to the interpretation of studies using this model, and may have implications for experimental therapeutics in ALI.

Materials & Methods

Animals and in vivo models

Male C57BL/6 and BALB/c mice were purchased from Jackson (Bar Harbor, ME). Mincle$^{-/-}$ mice were obtained from the MMRRC (San Diego, CA). Dectin-1$^{-/-}$ mice were a gift of Gordon Brown (University of Aberdeen, UK). Animals were bred in-house. Age-matched 8–10 week old male mice were used in all experiments. To induce Con-A hepatitis, mice were treated with Con-A (20μg/g, IV Sigma-Aldrich, St. Louis, MO) and sacrificed at various time intervals. For survival experiments, higher doses of Con-A (40μg/g) were used as previously reported[10]. Serum liver enzymes including alanine transaminase (ALT) and aspartate aminotransferase (AST) were measured using a commercial kit (Sigma-Aldrich). Core temperature was measured at various time-points using a rectal thermometer for rodents (Braintree Scientific, Braintree, MA). In select experiments, mice were pretreated 1 hour prior to Con-A injection with an i.p injection of either a α-Mincle mAb (6G5, 3.5 mg/kg, Invivogen, San Diego, CA), a Syk inhibitor (Piceatannol, 25 mg/kg, Sigma-Aldrich), Mincle ligand (TDB, 10 mg/kg, Invivogen), a HIF-1α inhibitor (LW6, 60 mg/kg, EMD Millipore, Billerica, MA), or a C/EBPβ inhibitor (Genistein, 6.5 mg/mouse, Sigma-Aldrich)[8, 11–15]. Bone marrow chimeric mice were generated as previously described[16]. Briefly, mice were anesthetized and irradiated (950 Rads), followed by i.v. transfer with 1×10^7 bone marrow cells from donor mice. Chimeric mice were used in experiments seven weeks later. To induce hepatic fibrosis, female mice were treated with thrice weekly injections of thioacetamide (TAA; 250 mg/kg; Sigma) for 12 weeks as described [17]. Animal procedures were approved by the New York University School of Medicine IACUC.

Human and murine cellular isolation

Murine hepatic non-parenchymal cells (NPC) were collected as previously described[17]. Briefly, the portal vein was cannulated and infused with 1% Collagenase IV (Sigma-Aldrich). The liver was then removed, minced, and filtered to obtain single cell suspensions. Hepatocytes were excluded with serial low speed (400 RPM) centrifugation followed by high speed (2000 RPM) centrifugation to isolate the NPC, which were then further enriched over a 40% Optiprep (Sigma) gradient. Human liver NPCs were isolated using the same protocol as we have described[18]. Human peripheral blood mononuclear cells (PBMC) were isolated by overlaying whole blood diluted 1:1 in PBS over an equal amount of Ficoll. The cells were then spun at 2100 RPM for 21 min at 20°C and the buffy coat was harvested to obtain the PBMC as we described[19].

Flow cytometry, cytokine, SAP130, and nitrite analysis

For flow cytometry, single-cell suspensions of NPC and PBMC were incubated with Fc blocking reagent (Biolegend, San Diego, CA) for 10 min followed by a 30 min incubation with fluorescently-conjugated mAbs directed against mouse Mincle (4A9; MBL International, Woburn, MA), CD45 (30-F11), Gr1 (RB6-8C5), CD11b (M1/70), CD11c (N418), MHC II (M5/114.15.2), CD146 (ME-9F1), CD45.2 (30-F11), CD45.1 (A20), CD3

(17A2), CD4 (GK1.5), or F4/80 (BM8) (all Biolegend, San Diego, CA). For intracellular staining, cells were incubated for 4–6 hours with Brefeldin A (1:1000) before permeabilization of cells, and staining with fluorescently conjugated p-Syk (moch1ct) and iNOS (CXFNT) (all eBioscience, San Diego, CA). Human liver NPC and PBMC were stained with mAbs directed against CD45 (HI30), CD15 (W6D3), Lin (CD3/14/19/20/56), HLA-DR (L243; all Biolegend), or Mincle (polyclonal; Abcam, Cambridge, MA). Experiments were performed using the LSRII (BD Biosciences, Franklin Lakes, NJ) and analyzed using FlowJo software (Tree Star, Ashland, OR). Serum cytokine levels were determined using a cytometric bead array according to the manufacturer's protocol (BD Biosciences). Hepatic levels of SAP130 were determined by ELISA (MyBioSource, San Diego, CA). Hepatic and serum nitrite levels were determined using the Griess assay (Life Technologies, Carlsbad, CA).

Histopathology and immunohistochemistry

For histological analysis, liver specimens were fixed with 10% buffered formalin, dehydrated in ethanol, and then embedded with paraffin and stained with hematoxylin-eosin (H&E) or Masson trichrome. Percent cell death was determined on a computerized grid as we have described[10]. For immunohistochemical analysis, slides were stained for anti-mouse CD45 (30-F11; BD Biosciences), MPO (polyclonal, Abcam), CD3 (17A2; Biolegend), CD68 (pAB; Abcam), p-Syk (polyclonal, Abcam), as well as anti-human Mincle (AT16E3, Abcam), SAP-130 (polyclonal, Abcam), and p-Syk (polyclonal, Abam). TUNEL staining was performed using a kit (EMD Millipore, Billerica, MA). For immunofluorescent imaging, murine $CD45^+$ NPCs were isolated using CD45 MicroBeads (Miltenyi, Bergisch Gladbach, Germany) stained for Mincle (CLEC-4E polyclonal, Santa Cruz Biotechnology, Dallas, TX) or p-Syk (polyclonal, Abcam), and then detected with donkey anti-goat IgG-PE, goat anti-rabbit IgG-Fitc (both Santa Cruz Biotechnology), and DAPI counterstain (Vector Laboratories, Burlingame, CA). Light microscopic images were captured with a Zeiss Axioscope 40 microscope/camera system (Zeiss, Thornwood, NY). Immunofluorescent imaging was performed using a LSM 700 confocal microscope and an Axiovert camera (Zeiss). Data was quantified by examining 10 high powered fields (HPFs) per slide.

Western Blotting and Immunoprecipitation

For Western blotting, total protein was isolated from 10mg liver tissue by homogenization in RIPA buffer (50 mM pH 7.4 Tris-Hcl, 150 mM NaCl, 0.5% Na-deoxycolate, 0.5% NP-40, 0.25% SDS, 5 mM EDTA) with Complete Protease Inhibitor cocktail (Roche, Pleasanton, CA). Proteins were separated from larger fragments by centrifugation at 14000 × g. After determining total protein by Bradford protein assay, 10% polyacrylamide gels (NuPage, Invitrogen, Grand Island, NY) were equiloaded, electrophoresed at 200V, electrotransferred to PVDF membranes, and probed with mAbs to p-Syk (C87C1), Syk (D321E), SAP-130 (H-300, Santa Cruz), Mincle (H-46, Santa-Cruz), and β-actin (13E5) (all Abcam). Blots were developed by ECL (Thermo Scientific, Ashville, NC). For immunoprecipitation experiments, SAP130 was precipitated with protein G-agarose from cells. Immunoprecipitates were re-suspended and heated in loading buffer under reduced conditions, and resolved by 10% SDS-PAGE before transfer to PVDF membranes. The presence of the co-immunoprecipitated Mincle was determined by Western blotting.

RNA Analysis

RNA extraction from whole liver tissues was performed using the RNeasy Mini kit (Qiagen, Germantown, MD) as per manufacturer's instructions. The RNA was converted to cDNA using the RT^2 First Strand Kit (Qiagen). qPCR was performed using the RT^2 SYBR Green qPCR mastermix (Qiagen) on the Stratagene MX3005P (Stratagene, La Jolla, CA). The mouse *tgf-β* primer was obtained from Qiagen (Cat # PPM02991B). Expression levels were normalized to β-actin. In selected experiments, the "Mouse Cytokine and Chemokine" pre-configured qPCR array was used (Qiagen). For Nanostring analysis, the nCounter mouse inflammation panel was employed using the nCounter Analysis System (both Nanostring, Seattle, Washington).

Statistical Analysis

Data is presented as mean +/− standard error of mean. Survival was measured according to the Kaplan-Meier method. Statistical significance was determined by the Student's *t* test and the log-rank test using GraphPad Prism 6 (GraphPad Software, La Jolla, CA). P-values of < 0.05 were considered significant.

Results

Mincle is highly expressed on hepatic inflammatory cells

Before investigating the role of Mincle signaling in Con-A hepatitis, we tested baseline Mincle expression in the liver. Murine liver non-parenchymal cells (NPC) expressed Mincle on immune fluorescence microscopy (Figure 1a). Flow cytometry revealed higher Mincle expression in liver $CD45^+$ pan-leukocytes, $Gr1^-CD11b^+F480^+$ macrophages, and $F480^-CD11c^+MHCII^+$ dendritic cells compared with their cellular counterparts in mouse spleen (Figure 1a). Liver sinusoidal endothelial cells (LSEC) also expressed high Mincle, whereas hepatocytes exhibited minimal expression (Figure 1b). Leukocytes and LSEC from $Mincle^{-/-}$ liver were used as controls (Figure S1a). Consistent with our mouse data, leukocytes in the human liver expressed Mincle on immune fluorescence microscopy (Figure 1c). Flow cytometry analysis in the human liver showed that hepatic $CD15^+$ monocytes and Lin^-HLADR^+ dendritic cells expressed substantially higher Mincle compared with their cellular counterparts in PBMC (Figure 1c, Figure S1b).

Con-A hepatitis is marked by SAP130 expression and Mincle signaling

To determine the relevance of Mincle signaling in murine Con-A hepatitis, we investigated Mincle expression, the presence of Mincle ligands, and associated downstream signaling intermediates in Con-A-treated mice. The rate of Mincle expression in hepatic leukocyte subsets was not significantly changed in Con-A hepatitis compared with control liver (Figure S1c). SAP130, the only well-characterized non-pathogen-derived Mincle ligand[8], was elevated in the liver of Con-A-treated animals on ELISA analysis (Figure 1d). SAP130 also co-associated with Mincle in Con-A hepatitis based on immunoprecipitation experiments (Figure 1e). Liver sections from mice with Con-A hepatitis also showed increased infiltration of cells expressing activated Syk (Figure 1f). Accordingly, Mincle and p-Syk co-localized in liver leukocytes (Figure S1d). Western blotting confirmed temporal

activation of Syk in the livers of Con-A-treated mice (Figures 1g). Similarly, analysis by flow cytometry confirmed elevated expression of p-Syk in liver inflammatory monocytes in Con-A hepatitis (Figures 1h). Collectively, these data confirm expression of Mincle, the presence of endogenous Mincle ligands, and activated downstream Mincle signaling intermediates in Con-A hepatitis.

Human autoimmune hepatitis is characterized by Mincle, SAP130, and p-Syk expression

ConA hepatitis is considered the best animal model of human autoimmune hepatitis[5]. Human autoimmune hepatitis was characterized by a marked infiltration of Mincle-expressing leukocytes (Figure S1e). SAP130 was similarly prevalent in the liver of patients with autoimmune hepatitis but absent in the uninjured liver (Figure S1f). Liver sections from patients with autoimmune hepatitis also showed increased infiltration of cells expressing activated Syk (Figure S1g). Collectively, these data confirm expression of Mincle, the presence of endogenous Mincle ligands, and activated downstream Mincle signaling intermediates in human disease and in murine models of autoimmune hepatitis.

Mincle deletion, blockade, or pathway inhibition protects against Con-A hepatitis

To test the significance of Mincle signaling in Con-A hepatitis, we treated WT and Mincle$^{-/-}$ mice with Con-A and harvested livers at serial intervals. Mincle$^{-/-}$ mice were protected, exhibiting only minimal hepatic necrosis and diminished numbers of TUNEL^{+} nuclear bodies (Figure 2a). Accordingly, Con-A-treated Mincle$^{-/-}$ mice exhibited significantly lower serum transaminase levels in comparison with WT (Figures 2b), lower serum levels of immune modulatory cytokines including TNF-α, IL-10, IFN-γ, IL-6, and MCP-1 (Figure 2c), and diminished hepatic expression of the pro-apoptotic genes FasL and Bcl2 (Figure 2d). Further, Mincle deletion resulted in a diminished reduction of core body temperature after Con-A challenge, indicative of lower systemic toxicity (Figure 2e). To determine whether Mincle deletion is protective against mortality from Con-A hepatitis, mice were administered a potentially lethal dose of Con-A and followed for 6 days after treatment or until moribund. Only ~40% of Mincle$^{-/-}$ mice succumbed to liver injury compared with a ~90% mortality rate in WT controls (Figure 2f). Notably, PBS-treated WT and Mincle$^{-/-}$ mice exhibited similar hepatic histology, serum transaminase levels, serum cytokine levels, core body temperatures, and hepatic inflammatory cell profiles (Figure S2).

We next tested whether Mincle blockade using a neutralizing mAb would similarly protect against Con-A hepatitis. Mice treated with α-Mincle were protected against Con-A-induced hepatic necrosis (Figure 3a) and exhibited a reduced elevation in serum cytokines (Figure 3b). Similarly, blockade of Syk signaling also protected against Con-A-induced hepatic necrosis (Figure 3c) and systemic toxicity (Figure 3d). Taken together, our data suggests that the full-extent of liver injury in Con-A hepatitis requires Mincle signaling.

Mincle ligation exacerbates Con-A hepatitis

To further test our hypothesis that Mincle signaling promotes liver injury and systemic toxicity in Con-A hepatitis, we investigated whether exogenous Mincle ligands would exacerbate Con-A-mediated liver injury. We treated WT mice with PBS, Mincle ligand TDB alone, Con-A alone, or TDB + Con-A. Consistent with our hypothesis, Mincle ligation

increased the extent of hepatic necrosis and the systemic toxicity associated with Con-A hepatitis (Figure 3e, f). Conversely, Mincle ligation alone, in absence of Con-A administration, had no effect. TDB administration did not exacerbate Con-A injury in Mincle$^{-/-}$ animals (not shown). Interestingly, Mincle deletion did not mitigate toxin-induced chronic liver fibrosis (Figure 4a–c).

Dectin-1 deletion does not protect against Con-A hepatitis

We next tested whether signaling via alternate C-type lectin receptors similarly modulates Con-A hepatitis. Dectin-1 is C-type lectin receptor which is similar to Mincle in that it also contains an ITAM-like motif in its intracellular tail and signals via p-Syk. Dectin-1 recognizes β-glucans found in fungal cell walls and is critical in anti-fungal immunity[20]. However, we recently reported that Dectin-1 has a central role in intra-hepatic sterile inflammation and promotes hepatic regeneration by binding intra-hepatic damage associated molecular patterns (DAMPs)[21]. Nevertheless, unlike the marked effects of Mincle blockade in Con-A hepatitis, deletion of Dectin-1 did not mitigate the hepatotoxic or pro-inflammatory effects of Con-A administration as measured by liver necrosis, serum transaminase levels, and serum cytokines (Figure 4d–f).

Mincle signaling in infiltrating myeloid cells governs Con-A hepatitis

Since Mincle is highly expressed in diverse hepatic leukocytes but absent in hepatocytes, we postulated that signaling via Mincle in liver-infiltrating inflammatory cells drives hepatic injury. To test this, we generated bone marrow chimeric Mincle$^{-/-}$ and WT animals in which Mincle is deleted in either bone-marrow derived inflammatory cells or in parenchymal and resident hepatic cells, respectively. Based on parallel experiments using CD45.1 congenic mice, our extent of chimerism was >95% (Figure 5a). WT mice made chimeric using Mincle$^{-/-}$ bone marrow (WT (Mincle$^{-/-}$)) were protected from Con-A hepatitis exhibiting reduced geographic areas of hepatic necrosis and lower TUNEL staining (Figure 5b), lower serum ALT (Figure 5c), reduced serum cytokines (Figure 5d), and a diminished reduction in core body temperature (Figure 5e). Conversely, Mincle$^{-/-}$ mice made chimeric using WT bone marrow (Mincle$^{-/-}$ (WT)) were not protected (Figure 5b–e). These data suggest that Mincle signaling specifically in the liver infiltrating inflammatory cells mediates hepatic injury in Con-A hepatitis. Further, adoptive transfer of CD11b^{+} myeloid cells from WT donors to Mincle$^{-/-}$ mice coincident with Con-A administration exacerbated disease phenotype compared with transfer of Mincle$^{-/-}$ myeloid cells (Figure 5f).

Mincle modulates intra-hepatic inflammation in Con-A hepatitis

To investigate the mechanism underlying Mincle modulation of Con-A hepatitis, we compared the intra-hepatic immune infiltrate in Con-A-treated WT and Mincle$^{-/-}$ hosts. Consistent with their exacerbated injury, WT mice exhibited a higher CD45^{+} pan-leukocyte infiltrate and increased intra-hepatic neutrophilia and CD3^{+} T cell influx (Figure 6a). Accordingly, levels of numerous bioactive chemokines, chemokine receptors, and inflammation-promoting transcription factors were reduced in Con-A-treated Mincle$^{-/-}$ liver compared with WT (Figure 6b). Conversely, TGF-β, which has potent anti-inflammatory properties, along with CCL8 and CXCL12, were elevated in Con-A-treated Mincle$^{-/-}$ liver (Figure 6b). Mincle$^{-/-}$ liver also had an increased influx of CD68^{+} macrophages as

compared to WT liver in Con-A hepatitis (Figure 6a). Flow cytometry analysis showed that intra-hepatic macrophages and the fraction of $Gr1^{int}CD11b^{+}$ monocytes were higher in the $Mincle^{-/-}$ liver, whereas the fraction of $CD3^{+}$ T cells and $Gr1^{hi}CD11b^{+}$ neutrophils was higher in the WT liver (Figures 6c). Further, WT mice had a higher CD4:CD8 ratio after Con-A treatment (Figures 6c). The cellular distribution of leukocytic subsets was similar at baseline in WT and $Mincle^{-/-}$ liver (Figure S2e).

Liver injury and inflammation in Con-A hepatitis is contingent on Mincle-dependent expression of HIF-1α and C/EBPβ

Since Mincle signaling was recently shown to mediate nitric oxide-dependent inflammatory responses to mycobacterial cord factor via HIF-1α and C/EBPβ[22], and expression of both HIF-1α and C/EBPβ was reduced in Con-A-treated $Mincle^{-/-}$ liver (Figure 6b), we postulated that hepatic injury in Con-A hepatitis may be dependent on these transcription factors. Accordingly, we found that nitrite levels were reduced in the liver and serum of Con-A-treated $Mincle^{-/-}$ animals compared with WT (Figure 6d). Further, we treated mice with selective inhibitors of either HIF-1α or C/EBPβ coincident with Con-A administration and found that HIF-1α and C/EBPβ blockade each protected WT mice from Con-A hepatitis, reducing cellular injury, intra-hepatic neutrophilia, and systemic inflammation (Figure 7a–d). Conversely, HIF-1α increased TGF-β expression, whereas C/EBPβ blockade significantly increased it (Figure 7e). HIF-1α and C/EBPβ inhibition had no discernable effect on modulating Con-A hepatitis in $Mincle^{-/-}$ animals (Figure S3). However, whereas $Gr1^{int}CD11b^{+}$ inflammatory moncoytes were increased after blockade of HIF-1α and C/EBPβ in Con-A hepatitis, which was similar to Mincle deletion, effects of HIF-1α or C/EBPβ inhibiton on $Gr1^{hi}CD11b^{+}$ neutrophils and $Gr1^{-}CD11b^{+}$ macrophages did not phenocopy the effects of Mincle deletion (Figure 7f). We confirmed that both HIF-1α and C/EBPβ blockade *in vivo* markedly lowered iNOS expression in hepatic inflammatory cells (Figure S4), which correlates with our data showing lower nitrite levels in Con-A-treated $Mincle^{-/-}$ animals (Figure 6d).

Discussion

Con-A hepatitis is a well-described murine model of acute hepatitis, which has been used to investigate both T-cell and cytokine-mediated liver injury[5]. Specifically, Con-A binds to and modifies MHC complexes on hepatic Kupffer cells leading to activation of $CD4^{+}$ T cells against hepatocytes. NKT cells have been also been implicated as mediators of hepatocyte cell death in this model[25, 26]. Moreover, the inciting $CD4^{+}$ T cell-mediated injury leads to a second hit" involving an array of innate inflammatory elements[23–25]. Ligation of select innate immune receptors, such as TLR9, by intra-hepatic DAMPs have been shown to exacerbate injury through cytokine release from hepatic macrophages and Kupffer cells[26–28]. Our study is the first to implicate the innate immune receptor Mincle in the pathogenesis of Con-A hepatitis, or in any model of acute liver injury, and suggests that targeting Mincle may be an attractive strategy for experimental therapeutics.

Mincle is a C-type lectin receptor, well characterized by its ability to bind mycobacterial cord factor Trehalose-6,6-dimycolate (TDM) – a glycolipid molecule found in the cell wall

of select mycobacteria – and has been implicated in the inflammatory response to diverse pathogens including *mycobacterium bovis*, *candida albicans* and *streptococcus pneumoniae*[11, 29–31]. Interestingly, akin to Con-A hepatitis, the immune response to each of these pathogenic entities is thought to be primarily T-cell mediated[32, 33]. In addition to ligating select pathogen-associated molecular patterns (PAMPs), Yamasaki et al. elegantly demonstrated that Mincle binds SAP130, a nuclear protein released from non-apoptotic dying cells, inducing p-Syk dependent inflammatory responses[8]. However, the only detailed investigations into a role for Mincle in non-pathogen induced sterile inflammation are in the context of ischemic brain injury and obesity-induced adipose tissue fibrosis. Specifically, Mincle expression was found to be upregulated during ischemic stroke, whereas inhibition of Mincle signaling via Syk blockade led to a significant decrease in the volume of cerebral infarct and brain swelling[34]. Similarly, Mincle signaling affects neuro-inflammation after subarachnoid hemorrhage and traumatic brain injury[35, 36]. Mincle deletion has also been shown to mitigate obesity-induced insulin resistance in mice fed high-fat diets[37]. However, little is known about the role of Mincle in sterile inflammation in clinical or pre-clinical models outside of these contexts.

We found that Mincle is highly expressed in liver APC in mice and in human liver $CD15^+$ monocytic cells and $Lin^-HLA^-DR^+$ dendritic cells. Further, both SAP130 and activated Mincle-associated signaling intermediates are over-expressed in Con-A hepatitis. Our lab has recently reported that necroptosis, an organized form of Caspase 8-independent cellular death requiring RIP1 and RIP3 co-localization, is the primary mode of cell death in murine Con-A hepatitis[10]. Therefore, we postulated that Mincle perpetuates insidious inflammatory liver injury by binding SAP130, released from necroptotic hepatocytes after the initial insult. We demonstrate that Mincle and SAP130 co-associate in Con-A hepatitis suggesting that the Mincle-SAP130 axis may be relevant in this disease model. It is notable that Mincle deletion did not influence toxin-induced liver fibrosis. However, it likely that chronic liver injury is not characterized by the same rate of necrotic or necroptotic cell death seen in acute injury precipitating Mincle ligation. Further, the fact that deletion of Dectin-1, an allied C-type lectin receptor, did not mitigate liver injury in ConA hepatitis is interesting. However, whereas we reported a role for Dectin-1 in modulating sterile inflammation by mitigating TLR4 signaling, in contrast to Mincle, Dectin-1 does not have an well-described role in ligating DAMPs as sterile ligands for Dectin-1 have not been well-characterized.

Akira et al. reported that Mincle expression is restricted to cells of the myelomonocytic lineage[38]. Accordingly, we found that myeloid cells transferred from WT donors negated the protection against Con-A hepatitis in $Mincle^{-/-}$ animals. Mincle expression was conspicuously absent in hepatocytes. However, we discovered robust expression of Mincle on LSEC which have an emerging role in Con-A hepatitis[39, 40]. Nevertheless, our bone-marrow chimeric experiments demonstrate that interruption of Mincle signaling on bone marrow-derived liver inflammatory cells is sufficient to induce protection in Con-A hepatitis. Besides suggesting that LSEC do not have a primary role in the exacerbated liver disease linked to Mincle signaling, these data also imply that radiation resistant hepatic macrophage subsets, which represent up to 40% of $F4/80^+$ liver cells, are not the primary effectors in Mincle-mediated hepatic insult in our model[41]. These finding are consistent with previous reports by our group and others that LSEC have anti-inflammaotry properties in a

number of experimental contexts [39–42]. Similarly, resident liver macrophages do not have the high pro-inflammatory phenotype of infiltrating monocyte derived macrophages [43].

We demonstrated that Mincle deletion or blockade results in diminished injury in Con-A hepatitis including lower transaminase and serum cytokine levels, diminished pan-leukocyte influx, decreased numbers of intra-hepatic neutrophils, and lower T cells. Interestingly, we found a paradoxical increase in macrophages and in inflammatory monocytes in Con-A injury in Mincle$^{-/-}$ liver. These may be related to a robust macrophage-driven hepatic regenerative response[44]. Accordingly, we discovered diminished hepatic expression of pro-apoptotic genes in Mincle$^{-/-}$ liver. Alternatively, the increase in hepatic macrophages in Con-A-treated Mincle$^{-/-}$ liver may reflect a compensatory increase in the bone-marrow infiltrating macrophage population. Regardless, our data showing that Mincle ablation leads to extended animal survival in Con-A hepatitis provides strong rationale for interrupting the Mincle signaling pathway as a novel approach to experimental therapeutics in liver disease.

The primary pathogenic mechanism underlying Con-A injury is believed to entail Con-A binding to MHC II complexes on hepatic APC, resulting in conformational change in MHC II leading to CD4$^+$ T cell auto-activation and proliferation, and subsequent liver injury through Th1 and Th17 cytokine responses[5]. We demonstrate that Mincle deletion leads to reduced CD4$^+$ T cell proliferation in the liver of Con-A-treated mice and that Mincle is critical in inducing diverse immunogenic cytokine production from CD4$^+$ T cells. Importantly, Con-A administration also induces APC to produce an array of pro-inflammatory cytokines and chemokines, thus aggravating liver injury[45]. Our data suggest that Mincle signaling may by critical for sustainable expression of soluble inflammatory mediators in Con-A hepatitis. Specifically, we performed mRNA-based array studies demonstrating that Con-A-treated Mincle$^{-/-}$ liver had significantly decreased levels of pro-inflammatory mediators with established pathogenic roles in liver injury. A number of the Mincle-dependent chemokines which we identified are chemotactic for T cells and have been implicated Con-A or other models of liver injury. For example, Ccl17, which was diminished in the context of Mincle deletion, is secreted by macrophages and recruits CD4$^+$ T cells to the sites of hepatic inflammation. Ccl2 and Ccl3 have been shown to promote hepatic fibrosis and inflammation by recruiting macrophages and increasing proliferation and migration of hepatic stellate cells[46–48]. Cxcl10, which we also showed is upregulated in a Mincle-dependent manner, is induced by IFN-γ and was recently shown to recruit monocytes, Th1 cells, and NK cells to the site of liver injury[46]. Cxcl10 levels have been shown to be elevated in patients with Con-A hepatitis, and are also pro-fibrotic[49–51]. Collectively, these data suggest that intra-hepatic Mincle signaling is critical in generating the hepatotoxic inflammatory environment distinctive of Con-A hepatitis. Besides governing pro-inflammatory chemokine levels, we also show that Mincle regulates suppressive cytokine expression in Con-A hepatitis as we found decreased production of TGF-β in livers of Con-A-treated Mincle$^{-/-}$ mice. Previous studies have shown that impaired TGF-β signaling increases susceptibility to Con-A hepatitis in mouse models[52]. Taken together, these findings suggest that Mincle signaling significantly modulates the inflammatory axis in Con-A liver injury. Considering that a number of inflammatory mediators linked to Mincle signaling reportedly exacerbate liver disease, it is likely that the observed Mincle-depedent effects are the result of a combined effects of these cytokines and chemokines.

However, definitive determination of the inflammatory mediators required for Mincle-mediated effects in ConA hepatitis requires more exact investigation.

Most notably, we found increased expression of C/EBPβ and HIF-1α mRNA in the liver of Con-A treated WT mice as compared to Mincle$^{-/-}$ mice. Our findings are consistent with a recent report which showed regulation of Mincle-dependent mycobacterial cord factor recognition and inflammatory responses by both C/EBPβ and HIF1α[22]. C/EBPβ is critical for macrophage-mediated pro-inflammatory function and is specifically required for increasing the expression of pro-inflammatory cytokines, including IL-4, IL-6, and TNF-α[53]. Conversely, macrophages deficient in C/EBPβ cannot terminally differentiate, and inflammatory monocytes deficient in C/EBPβ demonstrate accelerated apoptosis in vivo[54, 55]. Further, HIF-1α upregulates iNOS expression leading to nitric oxide production which is necessary for pro-inflammatory macrophage function[56]. Accordingly, nitric oxide has a well-described role in perpetuating Con-A-induced liver injury[57, 58]. Our data suggests that pharmacologic blockade of C/EBPβ and HIF-1α is protective in Con-A hepatitis and is associated with decreased iNOS expression in various leukocyte subtypes. Consistent with these data, we also show that Con-A-treated Mincle$^{-/-}$ mice have lower hepatic and serum levels of nitrite versus WT mice. Moreover, C/EBPβ and HIF-1α protect in a Mincle specific manner as inhibition of these transcription factors offers no additional protection in Mincle$^{-/-}$ liver.

Collectively, our data implicate a novel role for the C-type lectin receptor, Mincle, in Con-A hepatitis via modulation of chemokine-mediated inflammation and enhancement of T cell proliferation. Moreover, Mincle deletion, blockade, or pharmacologic inhibition of downstream signaling through p-Syk, C/EBPβ, or HIf-1α, may provide therapeutic promise in acute liver disease. However, a limitation to both the C/EBPβ and HIF-1α inhibitors are their pleotropic pharmacologic effects. For instance, Farooqi et.al demonstrated that Genistein interfers with the MAP kinase signaling by preventing ERK and p38 MAPK phosphorylation [59]. Won et.al demonstrated that the HIF-1α inhibitor LW6 reduces HIF-1α levels by inhibiting malate dehydrogenase and interfering with mitochondrial respiration[60]. In human activated T cells, LW6 has been shown to abrograte T cell proliferation by decreasing levels of glucose transporter-1, lactate dehydrogenase-A and other proteins involved in glucose metabolism [61]. Hence, our conclusions must be tempered in light of these off-target effects.

Supplementary Material

Refer to Web version on PubMed Central for supplementary material.

Acknowledgments

This work was supported by grants from the Americas Hepato-Pancreato-Biliary Association (SG), the NYU Langone Medical Center Physician-Scientist Training Program (ATH), the Society of University Surgeons Resident Scholar Award (ATH), the American Liver Foundation (ATH), the German Research Foundation (LS), and National Institute of Health Awards DK085278 (GM), CA168611 (GM), and CA193111 (GM and ATH).

References

1. Murphy N. An update in acute liver failure: when to transplant and the role of liver support devices. Clin Med (Lond). 2006; 6:40–6. [PubMed: 16521355]
2. Chun LJ, Tong MJ, Busuttil RW, Hiatt JR. Acetaminophen hepatotoxicity and acute liver failure. J Clin Gastroenterol. 2009; 43:342–9. [PubMed: 19169150]
3. Singanayagam A, Bernal W. Update on acute liver failure. Curr Opin Crit Care. 2015; 21:134–41. [PubMed: 25689127]
4. Khashab M, Tector AJ, Kwo PY. Epidemiology of acute liver failure. Curr Gastroenterol Rep. 2007; 9:66–73. [PubMed: 17335680]
5. Wang HX, Liu M, Weng SY, Li JJ, Xie C, He HL, Guan W, Yuan YS, Gao J. Immune mechanisms of Concanavalin A model of autoimmune hepatitis. World J Gastroenterol. 2012; 18:119–25. [PubMed: 22253517]
6. Heymann F, Hamesch K, Weiskirchen R, Tacke F. The concanavalin A model of acute hepatitis in mice. Lab Anim. 2015; 49:12–20. [PubMed: 25835734]
7. Brown GD. Sensing necrosis with Mincle. Nat Immunol. 2008; 9:1099–100. [PubMed: 18800160]
8. Yamasaki S, Ishikawa E, Sakuma M, Hara H, Ogata K, Saito T. Mincle is an ITAM-coupled activating receptor that senses damaged cells. Nat Immunol. 2008; 9:1179–88. [PubMed: 18776906]
9. Seifert L, Werba G, Tiwari S, Giao LyNN, Alothman S, Alqunaibit D, Avanzi A, Barilla R, Daley D, Greco SH, Torres-Hernandez A, Pergamo M, Ochi A, Zambirinis CP, Pansari M, Rendon M, Tippens D, Hundeyin M, Mani VR, Hajdu C, Engle D, Miller G. The necrosome promotes pancreatic oncogenesis via CXCL1 and Mincle-induced immune suppression. Nature. 2016
10. Deutsch M, Graffeo CS, Rokosh R, Pansari M, Ochi A, Levie EM, Van Heerden E, Tippens DM, Greco S, Barilla R, Tomkotter L, Zambirinis CP, Avanzi N, Gulati R, Pachter HL, Torres-Hernandez A, Eisenthal A, Daley D, Miller G. Divergent effects of RIP1 or RIP3 blockade in murine models of acute liver injury. Cell Death Dis. 2015; 6:e1759. [PubMed: 25950489]
11. Ishikawa E, Ishikawa T, Morita YS, Toyonaga K, Yamada H, Takeuchi O, Kinoshita T, Akira S, Yoshikai Y, Yamasaki S. Direct recognition of the mycobacterial glycolipid, trehalose dimycolate, by C-type lectin Mincle. J Exp Med. 2009; 206:2879–88. [PubMed: 20008526]
12. Cambien B, Millet MA, Schmid-Antomarchi H, Brossette N, Rossi B, Schmid-Alliana A. Src-regulated extracellular signal-related kinase and Syk-regulated c-Jun N-terminal kinase pathways act in conjunction to induce IL-1 synthesis in response to microtubule disruption in HL60 cells. J Immunol. 1999; 163:5079–85. [PubMed: 10528214]
13. Chau NM, Rogers P, Aherne W, Carroll V, Collins I, McDonald E, Workman P, Ashcroft M. Identification of novel small molecule inhibitors of hypoxia-inducible factor-1 that differentially block hypoxia-inducible factor-1 activity and hypoxia-inducible factor-1alpha induction in response to hypoxic stress and growth factors. Cancer Res. 2005; 65:4918–28. [PubMed: 15930314]
14. Akiyama T, Ishida J, Nakagawa S, Ogawara H, Watanabe S, Itoh N, Shibuya M, Fukami Y. Genistein, a specific inhibitor of tyrosine-specific protein kinases. J Biol Chem. 1987; 262:5592–5. [PubMed: 3106339]
15. Lee K, Kang JE, Park SK, Jin Y, Chung KS, Kim HM, Lee K, Kang MR, Lee MK, Song KB, Yang EG, Lee JJ, Won M. LW6, a novel HIF-1 inhibitor, promotes proteasomal degradation of HIF-1alpha via upregulation of VHL in a colon cancer cell line. Biochem Pharmacol. 2010; 80:982–9. [PubMed: 20599784]
16. Bedrosian AS, Nguyen AH, Hackman M, Connolly MK, Malhotra A, Ibrahim J, Cieza-Rubio NE, Henning JR, Barilla R, Rehman A, Pachter HL, Medina-Zea MV, Cohen SM, Frey AB, Acehan D, Miller G. Dendritic cells promote pancreatic viability in mice with acute pancreatitis. Gastroenterology. 2011; 141:1915–26. e1–14. [PubMed: 21801698]
17. Connolly MK, Bedrosian AS, Mallen-St Clair J, Mitchell AP, Ibrahim J, Stroud A, Pachter HL, Bar-Sagi D, Frey AB, Miller G. In liver fibrosis, dendritic cells govern hepatic inflammation in mice via TNF-alpha. J Clin Invest. 2009; 119:3213–25. [PubMed: 19855130]
18. Ibrahim J, Nguyen AH, Rehman A, Ochi A, Jamal M, Graffeo CS, Henning JR, Zambirinis CP, Fallon NC, Barilla R, Badar S, Mitchell A, Rao RS, Acehan D, Frey AB, Miller G. Dendritic cell

populations with different concentrations of lipid regulate tolerance and immunity in mouse and human liver. Gastroenterology. 2012; 143:1061–72. [PubMed: 22705178]

19. Rehman A, Hemmert KC, Ochi A, Jamal M, Henning JR, Barilla R, Quesada JP, Zambirinis CP, Tang K, Ego-Osuala M, Rao RS, Greco S, Deutsch M, Narayan S, Pachter HL, Graffeo CS, Acehan D, Miller G. Role of fatty-acid synthesis in dendritic cell generation and function. J Immunol. 2013; 190:4640–9. [PubMed: 23536633]
20. Taylor PR, Tsoni SV, Willment JA, Dennehy KM, Rosas M, Findon H, Haynes K, Steele C, Botto M, Gordon S, Brown GD. Dectin-1 is required for beta-glucan recognition and control of fungal infection. Nat Immunol. 2007; 8:31–8. [PubMed: 17159984]
21. Rao R, Graffeo CS, Gulati R, Jamal M, Narayan S, Zambirinis CP, Barilla R, Deutsch M, Greco SH, Ochi A, Tomkotter L, Blobstein R, Avanzi A, Tippens DM, Gelbstein Y, Van Heerden E, Miller G. Interleukin 17-producing gammadeltaT cells promote hepatic regeneration in mice. Gastroenterology. 2014; 147:473–84. e2. [PubMed: 24801349]
22. Schoenen H, Huber A, Sonda N, Zimmermann S, Jantsch J, Lepenies B, Bronte V, Lang R. Differential control of Mincle-dependent cord factor recognition and macrophage responses by the transcription factors C/EBPbeta and HIF1alpha. J Immunol. 2014; 193:3664–75. [PubMed: 25156364]
23. Fang X, Wang R, Ma J, Ding Y, Shang W, Sun Z. Ameliorated ConA-induced hepatitis in the absence of PKC-theta. PLoS One. 2012; 7:e31174. [PubMed: 22347449]
24. Higashimoto M, Sakai Y, Takamura M, Usui S, Nasti A, Yoshida K, Seki A, Komura T, Honda M, Wada T, Furuichi K, Ochiya T, Kaneko S. Adipose tissue derived stromal stem cell therapy in murine ConA-derived hepatitis is dependent on myeloid-lineage and CD4+ T-cell suppression. Eur J Immunol. 2013; 43:2956–68. [PubMed: 23934743]
25. Nakaya M, Hashimoto M, Nakagawa R, Wakabayashi Y, Ishizaki T, Takada I, Komai K, Yoshida H, Yoshimura A. SOCS3 in T and NKT cells negatively regulates cytokine production and ameliorates ConA-induced hepatitis. J Immunol. 2009; 183:7047–53. [PubMed: 19915050]
26. Jiang W, Sun R, Zhou R, Wei H, Tian Z. TLR-9 activation aggravates concanavalin A-induced hepatitis via promoting accumulation and activation of liver CD4+ NKT cells. J Immunol. 2009; 182:3768–74. [PubMed: 19265155]
27. Xiao X, Zhao P, Rodriguez-Pinto D, Qi D, Henegariu O, Alexopoulou L, Flavell RA, Wong FS, Wen L. Inflammatory regulation by TLR3 in acute hepatitis. J Immunol. 2009; 183:3712–9. [PubMed: 19710451]
28. Li X, Liu HC, Yao QY, Xu BL, Zhang SC, Tu CT. Quercetin Protects Mice from ConA-Induced Hepatitis by Inhibiting HMGB1-TLR Expression and Down-Regulating the Nuclear Factor Kappa B Pathway. Inflammation. 2015
29. Bugarcic A, Hitchens K, Beckhouse AG, Wells CA, Ashman RB, Blanchard H. Human and mouse macrophage-inducible C-type lectin (Mincle) bind Candida albicans. Glycobiology. 2008; 18:679–85. [PubMed: 18509109]
30. Schoenen H, Bodendorfer B, Hitchens K, Manzanero S, Werninghaus K, Nimmerjahn F, Agger EM, Stenger S, Andersen P, Ruland J, Brown GD, Wells C, Lang R. Cutting edge: Mincle is essential for recognition and adjuvanticity of the mycobacterial cord factor and its synthetic analog trehalose-dibehenate. J Immunol. 2010; 184:2756–60. [PubMed: 20164423]
31. Rabes A, Zimmermann S, Reppe K, Lang R, Seeberger PH, Suttorp N, Witzenrath M, Lepenies B, Opitz B. The C-type lectin receptor Mincle binds to Streptococcus pneumoniae but plays a limited role in the anti-pneumococcal innate immune response. PLoS One. 2015; 10:e0117022. [PubMed: 25658823]
32. Ashman RB, Farah CS, Wanasaengsakul S, Hu Y, Pang G, Clancy RL. Innate versus adaptive immunity in Candida albicans infection. Immunol Cell Biol. 2004; 82:196–204. [PubMed: 15061774]
33. Pietrella D, Rachini A, Pines M, Pandey N, Mosci P, Bistoni F, d'Enfert C, Vecchiarelli A. Th17 cells and IL-17 in protective immunity to vaginal candidiasis. PLoS One. 2011; 6:e22770. [PubMed: 21818387]

34. Suzuki Y, Nakano Y, Mishiro K, Takagi T, Tsuruma K, Nakamura M, Yoshimura S, Shimazawa M, Hara H. Involvement of Mincle and Syk in the changes to innate immunity after ischemic stroke. Sci Rep. 2013; 3:3177. [PubMed: 24212132]
35. He Y, Xu L, Li B, Guo ZN, Hu Q, Guo Z, Tang J, Chen Y, Zhang Y, Tang J, Zhang JH. Macrophage-Inducible C-Type Lectin/Spleen Tyrosine Kinase Signaling Pathway Contributes to Neuroinflammation After Subarachnoid Hemorrhage in Rats. Stroke. 2015; 46:2277–86. [PubMed: 26138128]
36. de Rivero Vaccari JC, Brand FJ 3rd, Berti AF, Alonso OF, Bullock MR, de Rivero Vaccari JP. Mincle signaling in the innate immune response after traumatic brain injury. J Neurotrauma. 2015; 32:228–36. [PubMed: 25111533]
37. Tanaka M, Ikeda K, Suganami T, Komiya C, Ochi K, Shirakawa I, Hamaguchi M, Nishimura S, Manabe I, Matsuda T, Kimura K, Inoue H, Inagaki Y, Aoe S, Yamasaki S, Ogawa Y. Macrophage-inducible C-type lectin underlies obesity-induced adipose tissue fibrosis. Nat Commun. 2014; 5:4982. [PubMed: 25236782]
38. Masumoto M, Tanaka T, Kaisho T, Sanjo H, Copeland NG, Gilbert DJ, Jenkins NA, Akira S. A novel LPS-inducible C-type lectin is a transcriptional target of NF-IL6 in macrophages. Journal of Immunology. 1999; 163:5039–5048.
39. Kruse N, Neumann K, Schrage A, Derkow K, Schott E, Erben U, Kuhl A, Loddenkemper C, Zeitz M, Hamann A, Klugewitz K. Priming of CD4+ T cells by liver sinusoidal endothelial cells induces CD25low forkhead box protein 3-regulatory T cells suppressing autoimmune hepatitis. Hepatology. 2009; 50:1904–13. [PubMed: 19787806]
40. Warren A, Bertolino P, Benseler V, Fraser R, McCaughan GW, Le Couteur DG. Marked changes of the hepatic sinusoid in a transgenic mouse model of acute immune-mediated hepatitis. J Hepatol. 2007; 46:239–46. [PubMed: 17125874]
41. Klein I, Cornejo JC, Polakos NK, John B, Wuensch SA, Topham DJ, Pierce RH, Crispe IN. Kupffer cell heterogeneity: functional properties of bone marrow derived and sessile hepatic macrophages. Blood. 2007; 110:4077–85. [PubMed: 17690256]
42. Neumann K, Rudolph C, Neumann C, Janke M, Amsen D, Scheffold A. Liver sinusoidal endothelial cells induce immunosuppressive IL-10-producing Th1 cells via the Notch pathway. Eur J Immunol. 2015; 45:2008–16. [PubMed: 25884798]
43. Heymann F, Peusquens J, Ludwig-Portugall I, Kohlhepp M, Ergen C, Niemietz P, Martin C, van Rooijen N, Ochando JC, Randolph GJ, Luedde T, Ginhoux F, Kurts C, Trautwein C, Tacke F. Liver inflammation abrogates immunological tolerance induced by Kupffer cells. Hepatology. 2015; 62:279–91. [PubMed: 25810240]
44. Taub R. Liver regeneration: from myth to mechanism. Nat Rev Mol Cell Biol. 2004; 5:836–47. [PubMed: 15459664]
45. Hatano M, Sasaki S, Ohata S, Shiratsuchi Y, Yamazaki T, Nagata K, Kobayashi Y. Effects of Kupffer cell-depletion on Concanavalin A-induced hepatitis. Cell Immunol. 2008; 251:25–30. [PubMed: 18374909]
46. Czaja AJ. Review article: chemokines as orchestrators of autoimmune hepatitis and potential therapeutic targets. Aliment Pharmacol Ther. 2014; 40:261–79. [PubMed: 24890045]
47. Heinrichs D, Berres ML, Nellen A, Fischer P, Scholten D, Trautwein C, Wasmuth HE, Sahin H. The chemokine CCL3 promotes experimental liver fibrosis in mice. PLoS One. 2013; 8:e66106. [PubMed: 23799074]
48. Seki E, De Minicis S, Osterreicher CH, Kluwe J, Osawa Y, Brenner DA, Schwabe RF. TLR4 enhances TGF-beta signaling and hepatic fibrosis. Nat Med. 2007; 13:1324–32. [PubMed: 17952090]
49. Antonelli A, Ferri C, Fallahi P, Ferrari SM, Frascerra S, Carpi A, Nicolini A, Ferrannini E. Alpha-chemokine CXCL10 and beta-chemokine CCL2 serum levels in patients with hepatitis C-associated cryoglobulinemia in the presence or absence of autoimmune thyroiditis. Metabolism. 2008; 57:1270–7. [PubMed: 18702954]
50. Lee EY, Lee ZH, Song YW. CXCL10 and autoimmune diseases. Autoimmun Rev. 2009; 8:379–83. [PubMed: 19105984]

51. Nishioji K, Okanoue T, Itoh Y, Narumi S, Sakamoto M, Nakamura H, Morita A, Kashima K. Increase of chemokine interferon-inducible protein-10 (IP-10) in the serum of patients with autoimmune liver diseases and increase of its mRNA expression in hepatocytes. Clin Exp Immunol. 2001; 123:271–9. [PubMed: 11207658]
52. Schramm C, Protschka M, Kohler HH, Podlech J, Reddehase MJ, Schirmacher P, Galle PR, Lohse AW, Blessing M. Impairment of TGF-beta signaling in T cells increases susceptibility to experimental autoimmune hepatitis in mice. Am J Physiol Gastrointest Liver Physiol. 2003; 284:G525–35. [PubMed: 12466145]
53. Rahman SM, Janssen RC, Choudhury M, Baquero KC, Aikens RM, de la Houssaye BA, Friedman JE. CCAAT/enhancer-binding protein beta (C/EBPbeta) expression regulates dietary-induced inflammation in macrophages and adipose tissue in mice. J Biol Chem. 2012; 287:34349–60. [PubMed: 22902781]
54. Ruffell D, Mourkioti F, Gambardella A, Kirstetter P, Lopez RG, Rosenthal N, Nerlov C. A CREB-C/EBPbeta cascade induces M2 macrophage-specific gene expression and promotes muscle injury repair. Proc Natl Acad Sci U S A. 2009; 106:17475–80. [PubMed: 19805133]
55. Tamura A, Hirai H, Yokota A, Sato A, Shoji T, Kashiwagi T, Iwasa M, Fujishiro A, Miura Y, Maekawa T. Accelerated apoptosis of peripheral blood monocytes in Cebpb-deficient mice. Biochem Biophys Res Commun. 2015; 464:654–8. [PubMed: 26168729]
56. Peyssonnaux C, Datta V, Cramer T, Doedens A, Theodorakis EA, Gallo RL, Hurtado-Ziola N, Nizet V, Johnson RS. HIF-1alpha expression regulates the bactericidal capacity of phagocytes. J Clin Invest. 2005; 115:1806–15. [PubMed: 16007254]
57. Fujita T, Soontrapa K, Ito Y, Iwaisako K, Moniaga CS, Asagiri M, Majima M, Narumiya S. Hepatic stellate cells relay inflammation signaling from sinusoids to parenchyma in mouse models of immune-mediated hepatitis. Hepatology. 2015
58. Tsuruoka N, Abe K, Wake K, Takata M, Hatta A, Sato T, Inoue H. Hepatic protection by glycyrrhizin and inhibition of iNOS expression in concanavalin A-induced liver injury in mice. Inflamm Res. 2009; 58:593–9. [PubMed: 19333727]
59. Ganai AA, Khan AA, Malik ZA, Farooqi H. Genistein modulates the expression of NF-kappaB and MAPK (p-38 and ERK1/2), thereby attenuating d-Galactosamine induced fulminant hepatic failure in Wistar rats. Toxicol Appl Pharmacol. 2015; 283:139–46. [PubMed: 25620059]
60. Lee K, Ban HS, Naik R, Hong YS, Son S, Kim BK, Xia Y, Song KB, Lee HS, Won M. Identification of malate dehydrogenase 2 as a target protein of the HIF-1 inhibitor LW6 using chemical probes. Angew Chem Int Ed Engl. 2013; 52:10286–9. [PubMed: 23934700]
61. Eleftheriadis T, Pissas G, Antoniadi G, Liakopoulos V, Stefanidis I. Malate dehydrogenase-2 inhibitor LW6 promotes metabolic adaptations and reduces proliferation and apoptosis in activated human T-cells. Exp Ther Med. 2015; 10:1959–1966. [PubMed: 26640580]

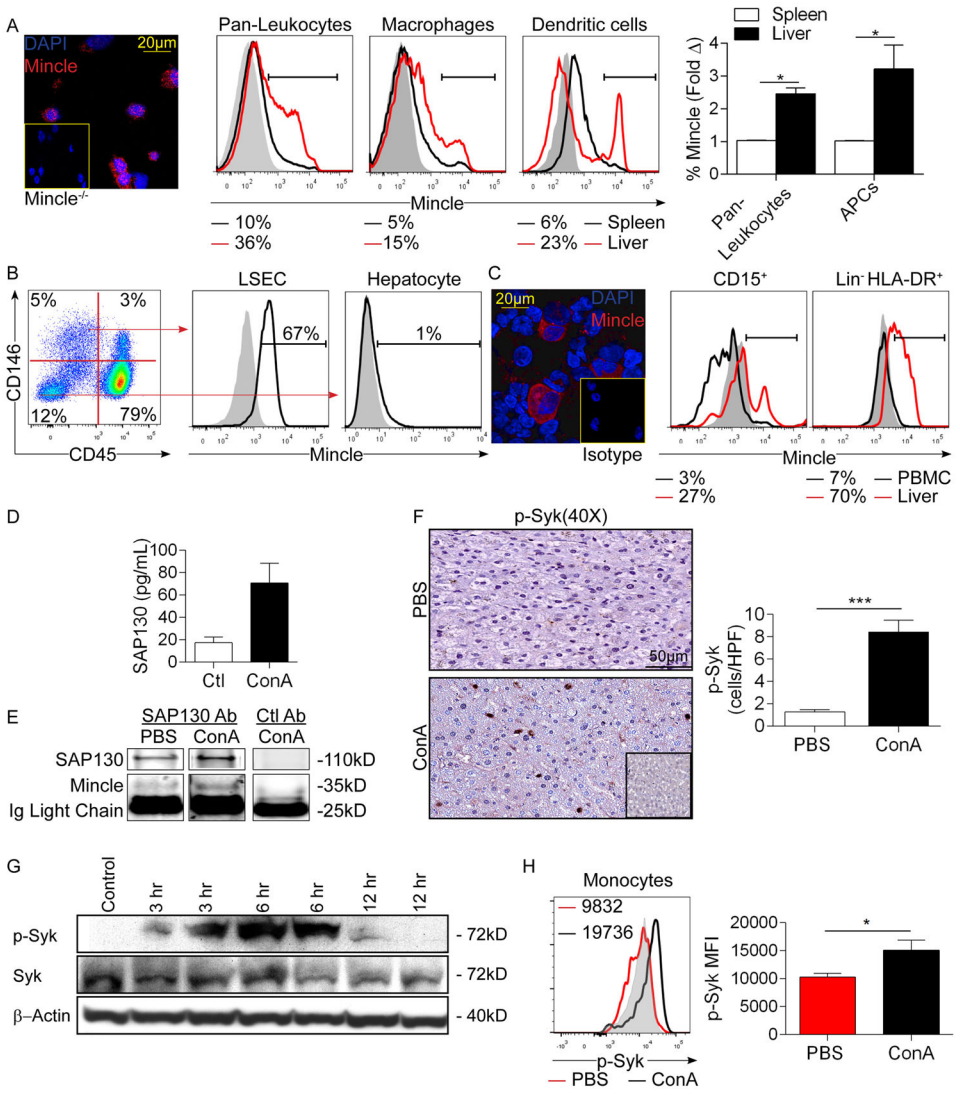

Figure 1. High Mincle expression and signaling in Con-A hepatitis

(a) Mincle expression was assayed in mouse liver NPC by confocal microscopy compared with NPC from Mincle$^{-/-}$ liver. Mincle expression was also compared by flow cytometry in mouse liver and spleen CD45^{+} pan-liver leukocytes, Gr1^{-}CD11b^{+}F480^{+} macrophages, and F480^{-}CD11c^{+}MHCII^{+} dendritic cells. Representative histograms and quantitative data from 4 mice are shown. Grey histograms represent isotype controls. **(b)** Mincle expression was tested in murine CD45^{-}CD146^{+} liver sinusoidal endothelial cells and CD45^{-}CD146^{-} hepatocytes by flow cytometry. Representative data indicating the percentage of positive cells relative to isotype control is shown. **(c)** Mincle expression was assayed in human liver NPC by confocal microscopy. Mincle expression was further tested by flow cytometry in human CD15^{+} liver monocytes and Lin^{-}HLA-DR^{+} liver dendritic cells compared with their counterparts in PBMC. Representative histograms are shown. Similar results were obtained from 5 separate patients. **(d)** Mice were treated with Con-A (20μg/g) or PBS and livers were harvested and tested for SAP130 expression by ELISA at 12h (n=3). **(e)** Lysates from PBS- or Con-A-treated mice were immuno-precipitated using an α-SAP130 or control mAb and

then tested for expression of SAP130 and Mincle. **(f)** Paraffin-embedded sections from livers of WT mice treated with PBS or Con-A were assayed for expression of p-Syk by immunohistochemistry at 12h. Isotype control is shown. Representative images and quantified data are shown (n=3/group). **(g)** The time course of Syk activation in Con-A hepatitis was tested by western blotting using liver lysate from 2 mice at each time point. β-actin was used as a loading control. **(h)** Inflammatory monocytes from the liver of PBS- and Con-A-treated mice were tested for expression of p-Syk at 12h after injury. Representative histograms and quantitative data from 3 mice based on median fluorescent indices (MFI) are shown (*p<0.05, ***p<0.001). All experiments were repeated at least twice with similar results.

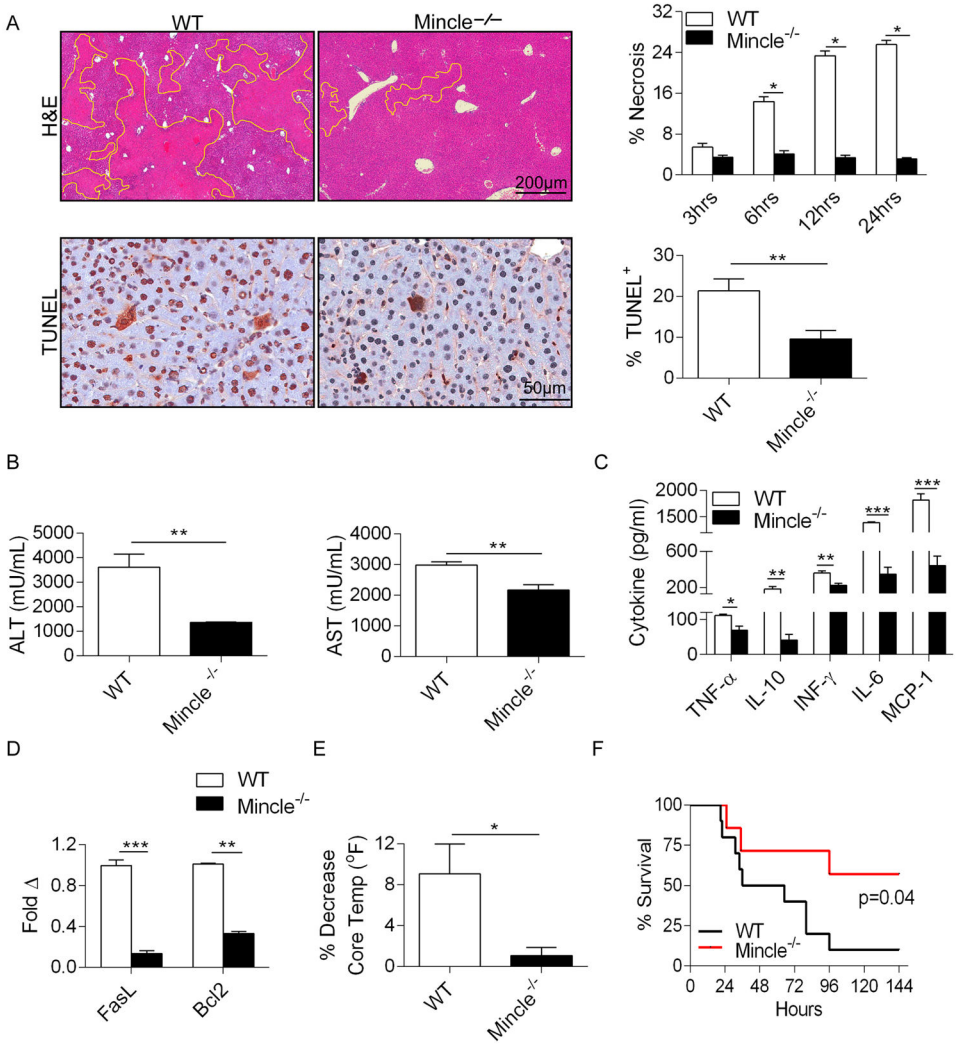

Figure 2. Mincle deletion is protective against Con-A hepatitis

WT and Mincle$^{-/-}$ mice were treated with Con-A (20μg/g; n=5/group). **(a)** Livers were harvested at serial time intervals and examined by H&E staining. The fraction of non-viable liver area was bracketed and calculated by examining 10 HPFs per liver. Representative H&E-stained sections from the 12h time-point are shown. Paraffin-embedded sections from the 12h time-point were also examined by TUNEL staining. The fraction of TUNEL^{+} hepatocytes was calculated. **(b)** Serum levels of ALT and AST, **(c)** TNF-α, IL-10, IFN-γ, IL-6, and MCP-1 were calculated for each cohort at 12h. **(d)** Similarly, hepatic expression of FasL and Bcl2 were calculated by a Nanostring assay. **(e)** The decrease in mouse rectal temperature from baseline was calculated at 12h in the WT and Mincle$^{-/-}$ cohorts. Experiments were repeated more than 5 times with similar results (*p<0.05, **p<0.01, ***p<0.001). **(f)** WT and Mincle$^{-/-}$ mice were treated with a potentially lethal dose of Con-A (40μg/g) and survival was measured according to the Kaplan-Meier method (n=10–11/group; p=0.04).

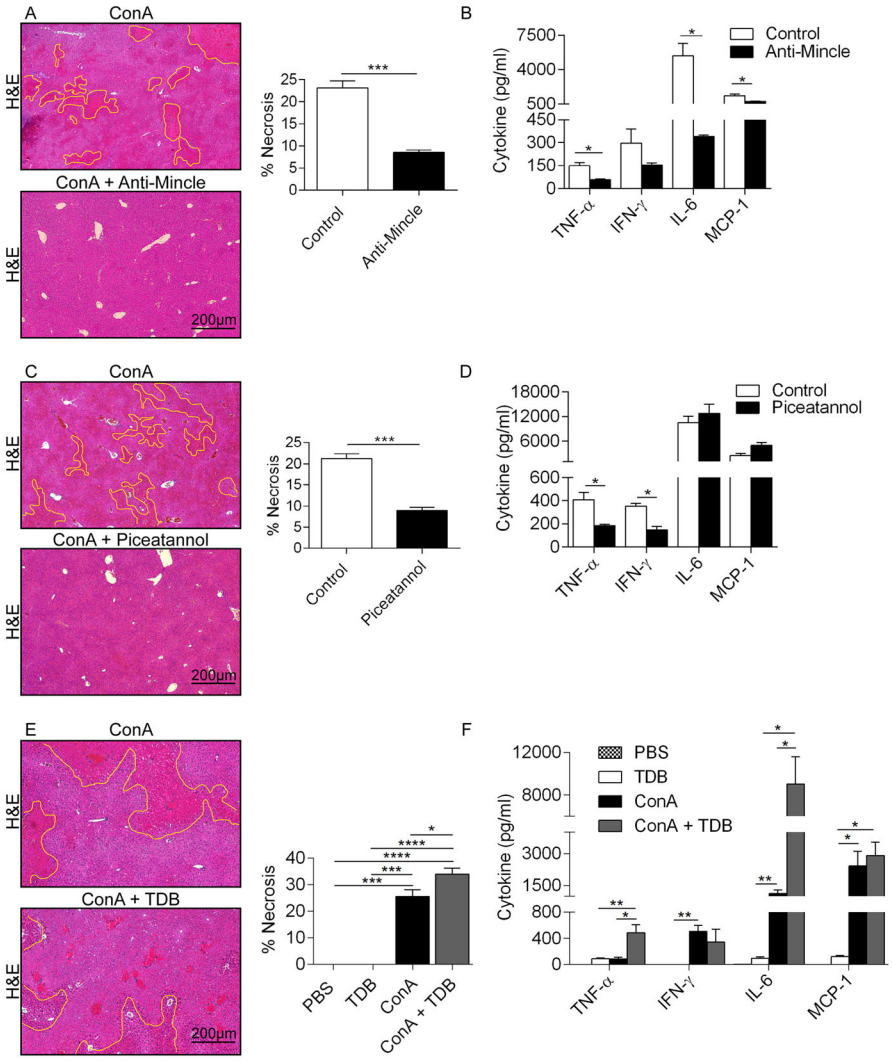

Figure 3. Mincle or Syk blockade are protective in Con-A hepatitis but Mincle ligation exacerbates disease

(a, b) WT mice were treated with Con-A alone or in combination with a neutralizing α-Mincle mAb (n=5/group). (a) Livers were harvested at 12h and the fraction of necrotic liver area was calculated based on H&E staining. (b) Serum levels of pro-inflammatory cytokines were tested. **(c, d)** WT mice were treated with Con-A alone or in combination with the Syk inhibitor Piceatannol (n=5/group). (c) Livers were harvested at 12h and the fraction of necrotic liver area was calculated based on H&E staining. (d) Serum levels of pro-inflammatory cytokines were tested. **(e, f)** WT mice were treated with PBS, TDB alone, Con-A alone, or Con-A + TDB (n=5/group). (e) Livers were harvested at 12h and the fraction of necrotic liver area was calculated based on H&E staining. (f) Serum levels of pro-inflammatory cytokines were tested (*p<0.05, **p<0.01, ***p<0.001, ****p<0.0001).

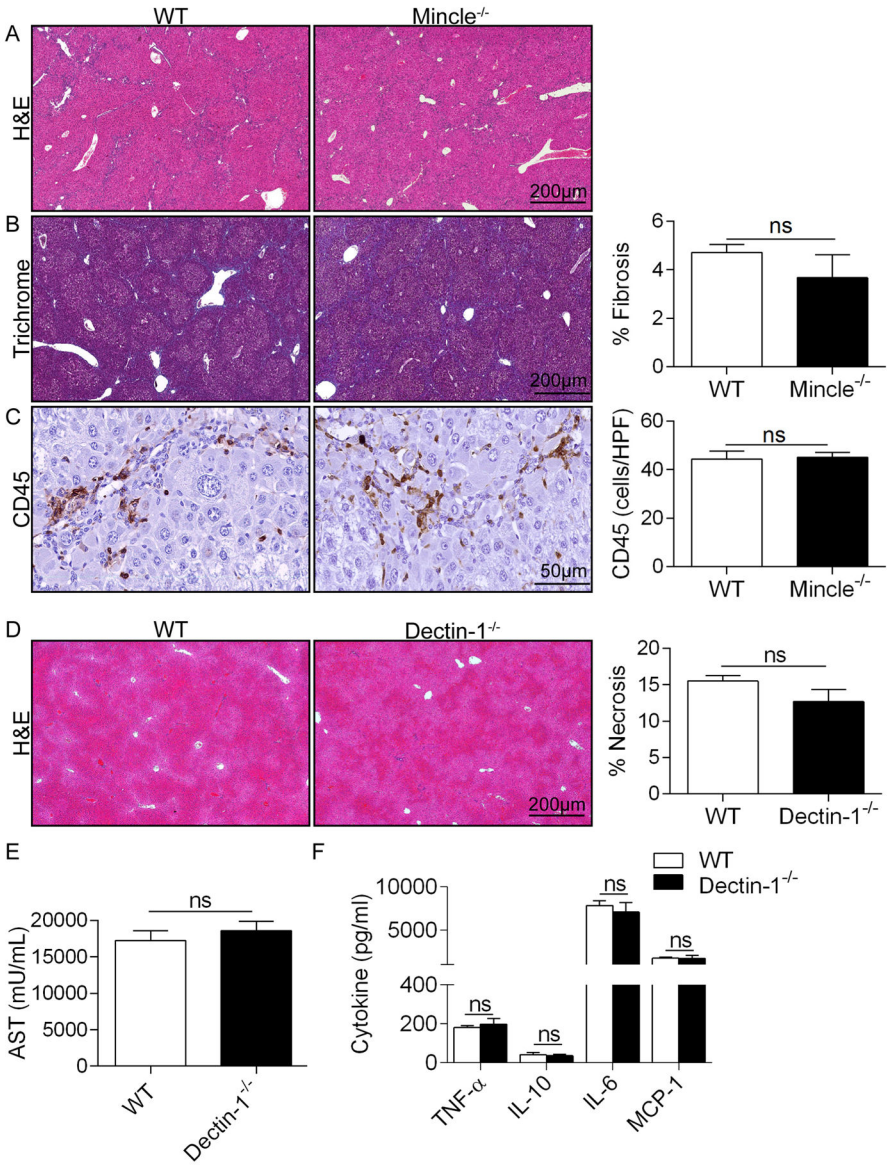

Figure 4. Mincle deletion does not mitigate TAA-induced liver fibrosis and Dectin-1 deletion does not protect against ConA hepatitis

(a–c) WT and Mincle$^{-/-}$ mice (n=5/group) were serially treated with TAA for 12 weeks. Livers were examined by (a) H&E and (b) trichrome staining and the percent fibrotic area was calculated. (c) CD45^{+} pan-leukocyte infiltrate were determined by immunohistochemistry. **(d–f)** WT and Dectin-1$^{-/-}$ mice were treated with Con-A (20μg/g). (d) Livers were harvested at 12h and examined by H&E staining. Representative H&E-stained sections are shown and the fraction of non-viable liver was calculated. (e) Serum levels of AST, (f) TNF-α, IL-10, IL-6, and MCP-1 were calculated for each cohort (n=5 group; p=ns for all comparisons). *In vivo* experiemnts were repeated twice with similar results.

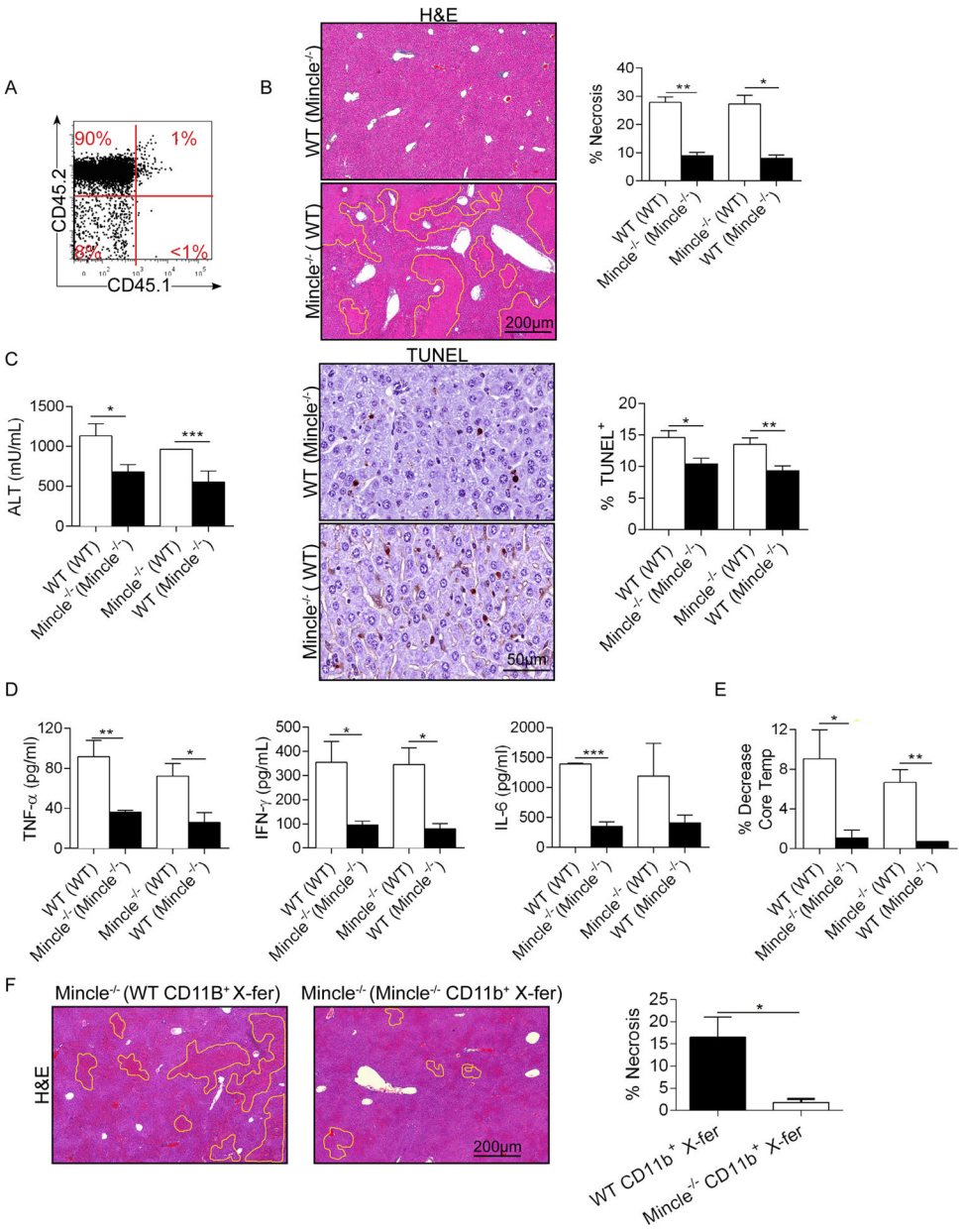

Figure 5. Mincle signaling in liver infiltrating inflammatory cells modulates Con-A hepatitis

(a) CD45.1 mice were irradiated and made chimeric with bone marrow derived from congenic CD45.2 mice. The extent of chimerism was tested at 7 weeks by flow cytometry and found to be near-complete. **(b)** WT mice were made chimeric with WT bone marrow 'WT (WT)' or Mincle$^{-/-}$ bone marrow 'WT (Mincle$^{-/-}$)'. Similarly, Mincle$^{-/-}$ mice were made chimeric with WT bone marrow 'Mincle$^{-/-}$ (WT)' or Mincle$^{-/-}$ bone marrow 'Mincle$^{-/-}$ (Mincle$^{-/-}$)'. Seven weeks later, all four cohorts were treated with Con-A (20μg/g; n=5/group). Livers were harvested at 12h and the percentage of non-viable liver was calculated based on H&E staining. Hepatocyte apoptosis was determined by TUNEL staining. **(c)** Serum ALT was calculated. **(d)** Serum TNF-α, IFN-γ, and IL-6 were measured. **(e)** The decrease in mouse rectal temperature from baseline was calculated for each cohort.

(f) Mincle$^{-/-}$ mice were adoptively transferred one hour prior to Con-A administration with CD11b^{+} hepatic leukocytes (1×10^{6} cells, i.v.) harvested from either WT or Mincle$^{-/-}$ liver. Mice were sacrificed at 12h and the percentage of non-viable liver was calculated based on H&E staining (*$p<0.05$, **$p<0.01$, ***$p<0.001$).

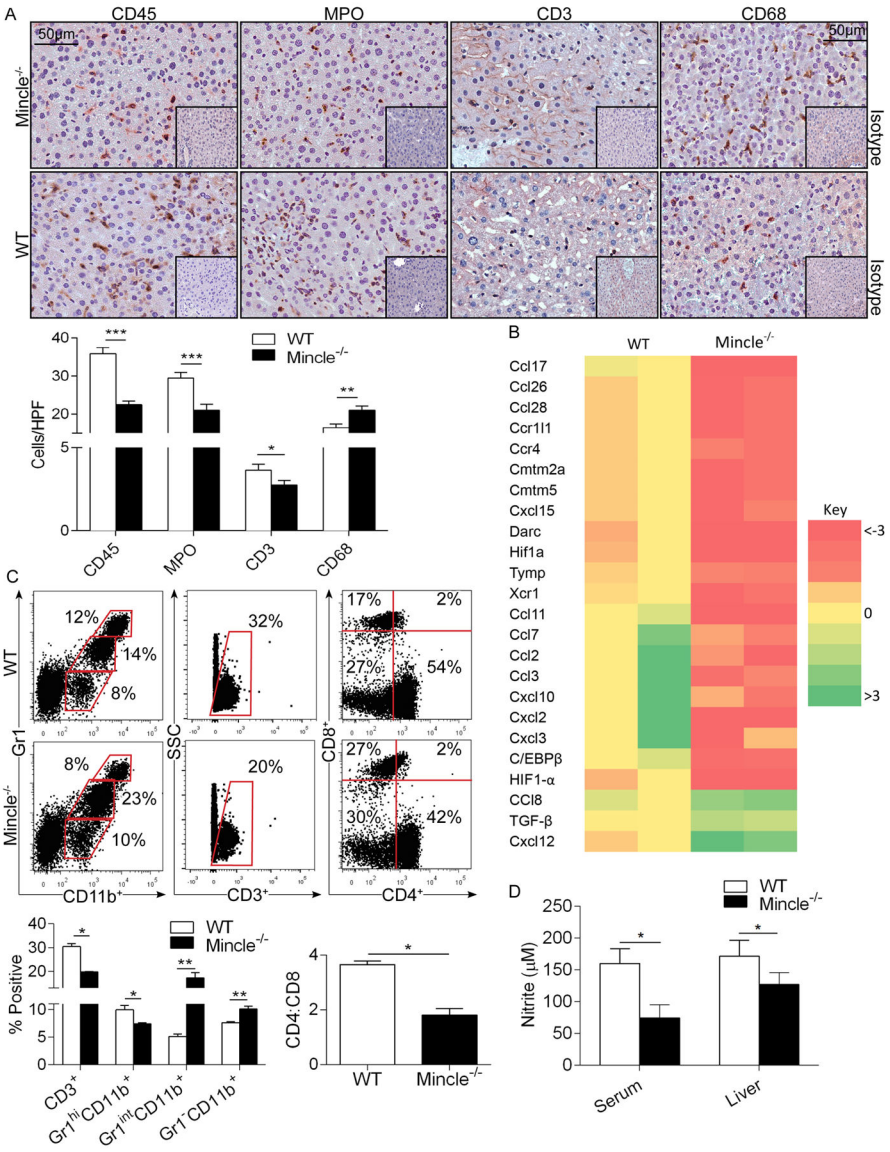

Figure 6. Mincle deletion modulates intra-hepatic inflammation and nitrite production in Con-A hepatitis

(a–c) WT and Mincle$^{-/-}$ mice were treated with Con-A (20μg/g). (a) CD45^{+} pan-leukocyte, MPO^{+} neutrophil, CD3^{+} T cell, and CD68^{+} macrophage infiltrate were determined by immunohistochemistry at 12h. Results were quantified by examining 10 HPFs per slide (n=5/group). (b) Intra-hepatic inflammation was determined by mRNA levels of diverse inflammatory mediators in whole liver tisues. A heat map analysis showing fold change in Mincle$^{-/-}$ mRNA expression levels relative to WT controls is shown (n=2/group). (c) Cellular ractions of myeloid and T cell subsets in livers of Con-A-treated WT and Mincle$^{-/-}$ mice were determined by flow cytometry. Representative dot plots and quantifications based on replicates, including the CD4:CD8 ratio, are shown. Flow cytometry experiments were reproduced more than 3 times using 3–5 mice per cohort. **(d)** The Griess assay was used to

determine nitrite levels in the liver and serum of WT and Mincle$^{-/-}$ mice at 12h after Con-A administration. (n=5/group; *p<0.05, **p<0.01, ***p<0.001).

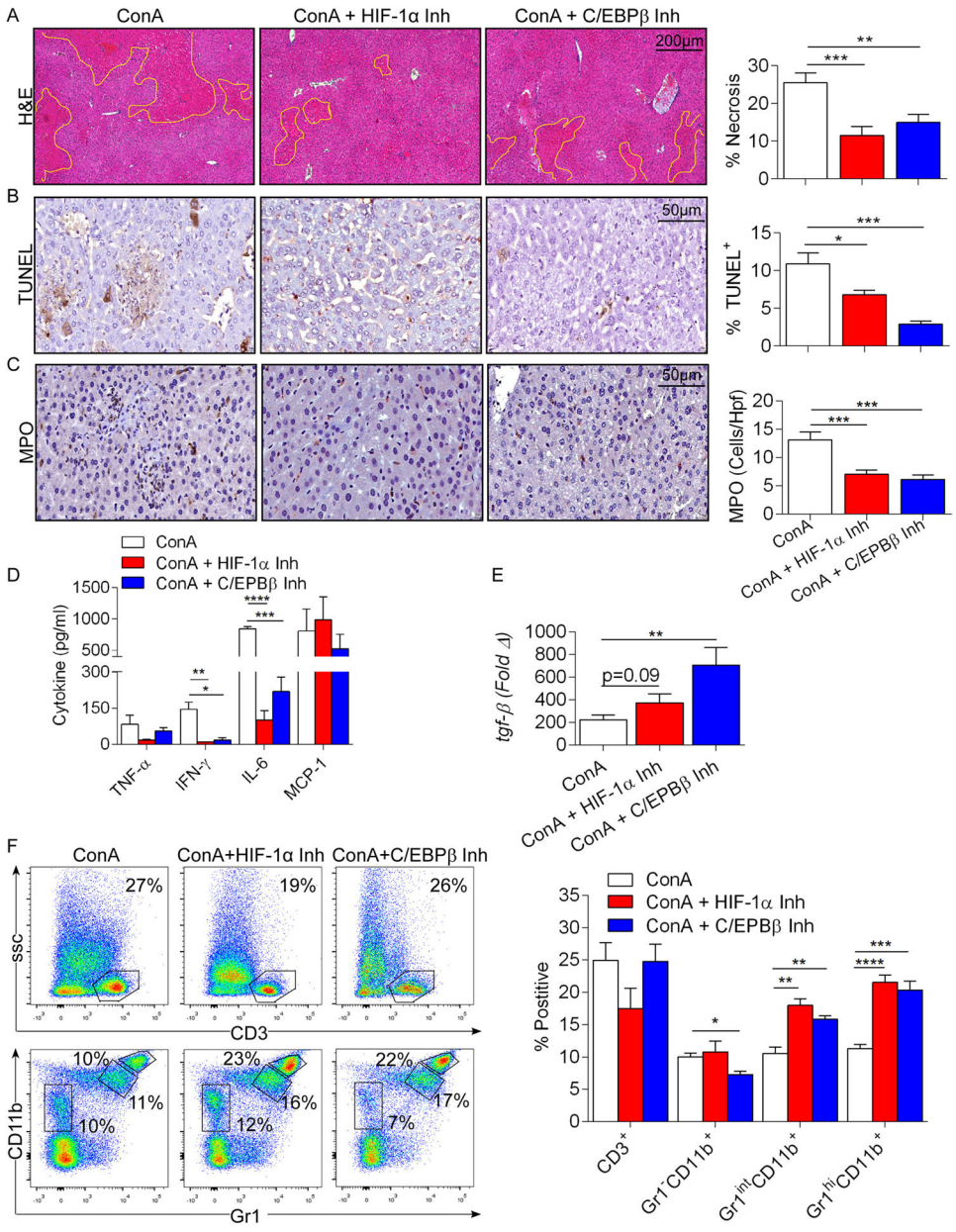

Figure 7. Inhibition of HIF-1α or C/EBPβ is protective against Con-A hepatitis

(a–e) WT mice were treated with Con-A (20μg/g) alone or in combination with a HIF-1α or C/EBPβ inhibitor. Injury was determined by (a) the percent necrotic liver area based on H&E staining, (b) the percentage of TUNEL$^+$ hepatocytes, (c) number of infiltrating MPO$^+$ cells, and (d) serum levels of TNF-α, IFN-γ, IL-6, and MCP-1. (e) Hepatic expression of TGF-β was tested at 12h by qPCR. Data was normalized to PBS-treated controls. (f) Cellular fractions of T cells and myeloid cellular subsets in livers of mice in each cohort were determined by flow cytometry. Representative pseudocolor plots and quantifications based on replicates are shown. This experiment was repeated twice (n=5/group; *p<0.05, **p<0.01, ***p<0.001, ****p<0.0001).